Rapid Communications

Projective cooling for the transverse Ising model

Erik J. Gustafson

Department of Physics and Astronomy, The University of Iowa, Iowa City, Iowa 52242, USA

(Received 2 March 2020; accepted 16 April 2020; published 28 April 2020)

We demonstrate the feasibility of ground state preparation for the transverse Ising model using projective cooling, and show that the algorithm can effectively construct the ground state in the disordered (paramagnetic) phase. On the other hand, significant temperature effects are encountered in the ordered (ferromagnetic) phase requiring larger lattices to accurately simulate.

DOI: 10.1103/PhysRevD.101.071504

I. INTRODUCTION

In quantum computing efficient state preparation methods are important for the analysis of quantum field theories so that field excitations can be accurately described. Much work has been done on constructing algorithms to prepare ground states and excited states for interacting field theories, and are briefly discussed to highlight their differences.

Quantum adiabatic evolution [1–3] involves slowly turning on some coupling in a model by real-time evolution to transform a state in a noninteracting theory to a corresponding state in the interacting theory. While this method is almost guaranteed to generate the correct state, the preparation of the state can take up the bulk of the quantum circuit. Quantum variational methods [4–6] are a hybrid algorithm which use a quantum computer to prepare and calculate the expectation value of the Hamiltonian of a chosen *Ansatz*, and then feed the result to a classical computer to minimize energy with respect to the parameters governing the *Ansatz*. The downside to variational methods is that improved *Ansätze* will often require more parameters and this leads to a classical minimization bottleneck.

Quantum phase estimation [7,8] works by applying iterative controlled time evolution operations a quantum state that is relatively close to the desired state. This method suffers from the same problem of circuit depth as quantum adiabatic evolution. Tensor networks can also be used for quantum computations [9], and do have similar strengths in approaching exact states; however, they are troubled by entanglement requirements and very deep quantum circuits. These issues make them intractable in the current era of noisy quantum computers. More recently, the authors of [10,11] suggested circumventing this problem by using classically generated lattice configurations, using Monte Carlo techniques, to construct the density matrix of the quantum system and perform time evolution on these states. Unlike the other methods, this one encounters a signal-to-noise problem; however, the authors demonstrated that it is mitigable. Another recently proposed algorithm, projective cooling, uses time evolution and selected qubit measurement to remove the high energy excitations of a Hamiltonian [12]. The first four algorithms each have their strengths and weaknesses in the field of quantum computing that have been thoroughly examined; however, not much work has focused on the strengths and weaknesses of projective cooling.

The work done in [12] investigated models which conserved particle number. The authors demonstrated that their new algorithm is efficient in preparing bound states for these Hamiltonians, and approached the correct bound state faster than adiabatic evolution. A natural extension is to examine a quantum field theory which has an effective "pair" creation and annihilation, the transverse Ising model (TIM). This choice is inspired by the road map used to develop lattice computations for QCD [13,14], since it is a stepping stone toward understanding theories containing confinement or are strongly coupled.

Section II layouts out the projective cooling algorithm and the Hamiltonian that will be investigated. Section III shows the results for the asymptotic behavior for both the ordered and disordered phases, and finite size scaling behavior in the transverse Ising model.

II. THEORY

The idea behind projective cooling involves removing high energy excitations outside of some region of interest by projecting them away. More explicitly, projective cooling works as follows (see Ref. [12] for more thorough details): a small region R_s, which contains N_s sites and supports the Hamiltonian of interest H_s, is chosen so that it is symmetrically contained within some larger system R_b (see Fig. 1), which contains N_b sites, with a corresponding

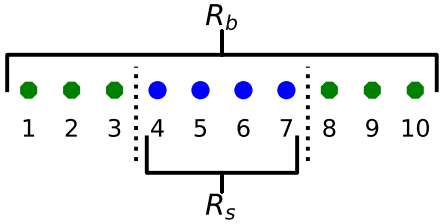

FIG. 1. Depiction of the regions R_b and R_s for a lattice with $N_b = 10$ total sites and an $N_s = 4$ sites contained within R_s. In this case $N_1 = 4$ and $N_2 = 7$.

Hamiltonian $\hat{H}_b$. An initial vector state $|\psi\rangle$ that has support on R_s is prepared on the quantum computer, and time evolved corresponding to $\hat{H}_b$. This process is in may ways similar to the quantum Joule expansion [15] where particle excitations are allowed to escape into a larger system after the walls constraining them are removed. The difference arises when the particle excitations outside of the R_s are projected away, and in the limit that $N_b \gg N_s$ the wave function in R_s will approach an asymptotic state. This algorithm can be summarized algebraically,

$$|\psi_0\rangle = \mathcal{P}U(t)|\psi\rangle, \tag{1}$$

where $\mathcal{P}$ is the operator that projects away excitations outside of the R_s, $U(t) = e^{-it\hat{H}_b}$, and $|\psi\rangle$ is the initial wave function. The projection operator $\mathcal{P}$ can be implemented by measuring the qubits outside of R_s and only keeping the result is if the state $|0\rangle$ is measured on all the qubits. This will encounter a sampling problem but is manageable in the near-term intermediate scale quantum (NISQ) era.

Two formulations for the TIM Hamiltonian were used in this work, depending on the quantum phase the system is in. The reason for choosing different formulations is a result of choosing a basis which is natural to work in. In the disordered phase ($J < h_T$), it is easier to work in a basis where the transverse field is diagonal; conversely, in the ordered phase ($J > h_T$) it is easier to work in a basis where the nearest neighbor coupling is diagonal. In the disordered phase, the formulation of the TIM Hamiltonian, in R_s, used in this work is

$$\hat{H}_s = -J\sum_{i=N_1}^{N_2-1}\hat{\sigma}_i^x\hat{\sigma}_{i+1}^x - \sum_{i=N_1}^{N_2}(h_T\hat{\sigma}_i^z + h\hat{\sigma}_i^x) \tag{2}$$

where J is the nearest neighbor coupling, h_T is the onsite energy, h is the longitudinal field coupling which lifts the degeneracy in the strongly ordered phase ($h_T = 0$), $N_1 = (N_b - N_s)/2 + 1$, and $N_2 = (N_b + N_s)/2$. It should be noted that N_b and N_s must have the same parity. This choice of N_1 and N_2 forces R_s to be symmetrically located within R_b. In this work $h_T = 1$, and $h = N_s^{-15/8}$ to ensure that the longitudinal field is perturbative. The choices of h_T and h are not arbitrary. Since the TIM undergoes a second order phase transition when $J = h_T$, setting $h_T = 1$ has the phase transition occur at $J = 1$. The choice of $h = h'(N_s)^{-15/8}$, where $h' = 1$, is to ensure that finite size scaling relations are obeyed, and the effects of the longitudinal field are perturbative. The factor of $15/8$ arises as a critical exponent for spacial correlation functions [16]. Reference [15] showed that in using this formulation for the TIM, finite size scaling relations were obeyed even for small lattices of eight sites. The Hamiltonian for R_b in the disordered phase is

$$\hat{H}_b = \hat{H}_s - J\sum_{i=1}^{N_1-1}(\hat{\sigma}_i^x\hat{\sigma}_{i+1}^x + \hat{\sigma}_i^y\hat{\sigma}_{i+1}^y) - J\sum_{i=N_2}^{N_b-1}(\hat{\sigma}_i^x\hat{\sigma}_{i+1}^x + \hat{\sigma}_i^y\hat{\sigma}_{i+1}^y) - h_T\sum_{i\notin R_s}\hat{\sigma}_i^z. \tag{3}$$

The introduction of the $\sigma_i^y\sigma_{i+1}^y$ terms outside of R_s and the exclusion of the longitudinal field σ_i^x is done to ensure no particles are created outside of R_s and "leak" back in, while the transverse field terms σ_i^z are kept to force spin down states to be more energetic than spin up states and force the state with all spins pointing down to be the ground state outside of R_s.

The ordered phase of the Hamiltonian is

$$\hat{H}_b = -J\sum_{i=1}^{N_b-1}\hat{\sigma}_i^z\hat{\sigma}_{i+1}^z - \sum_{i=1}^{N_b}(h_T\hat{\sigma}_i^x + N_b^{-15/8}\hat{\sigma}_i^z). \tag{4}$$

This Hamiltonian does not have a change in couplings to ensure that the domain wall excitations do not bounce back into R_s [17]; the risk of doing this is that there may be some "heat" leaking from outside R_s; however, later results will show that this is negligible.

In all cases, N_b ranges from 6 to 14, N_s ranges from 4 to 9 sites, and the initial state has all spins pointing up. Because of the size of some of the Hilbert spaces, the time evolution operator $U(t)$ is represented using a Suzuki-Trotter approximation; in the disordered phase the time evolution operator is

$$\hat{U}(t;\delta t) \approx \left(e^{i\delta tJ\sum_i\hat{\sigma}_i^y\hat{\sigma}_{i+1}^y}e^{i\delta tJ\sum_i\hat{\sigma}_i^x\hat{\sigma}_{i+1}^x}e^{i\delta th_T\sum_i\hat{\sigma}_i^z}e^{ih\delta t\sum_i\hat{\sigma}_i^x}\right)^{\frac{t}{\delta t}}, \tag{5}$$

while in the ordered phase the time evolution operator is

$$\hat{U}(t;\delta t) \approx \left(e^{i\delta tJ\sum_i\hat{\sigma}_i^z\hat{\sigma}_{i+1}^z}e^{i\delta th_T\sum_i\hat{\sigma}_i^x}e^{ih\delta t\sum_i\hat{\sigma}_i^z}\right)^{\frac{t}{\delta t}} \tag{6}$$

In all cases $\delta t = 0.01/J$ so as to keep the systematic error from this approximation negligible for large timescales.

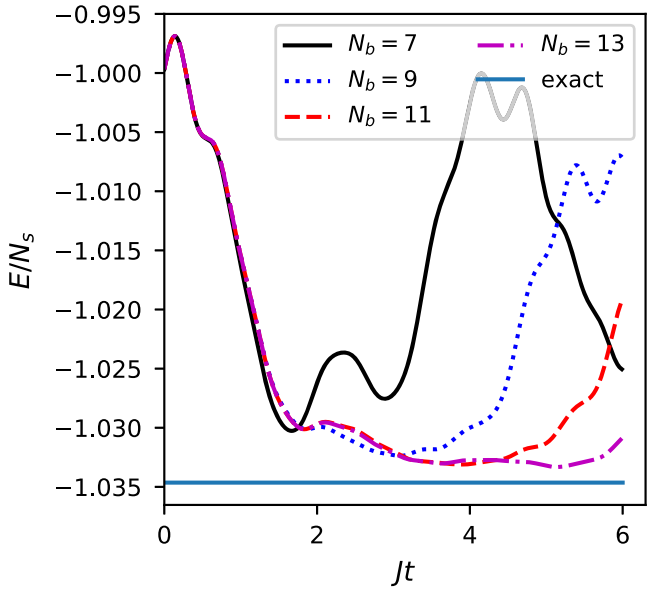

FIG. 2. Energy per site (in the small region) of projectively cooled state as a function of time in the ordered phase; $J = 0.4$, $N_s = 5$.

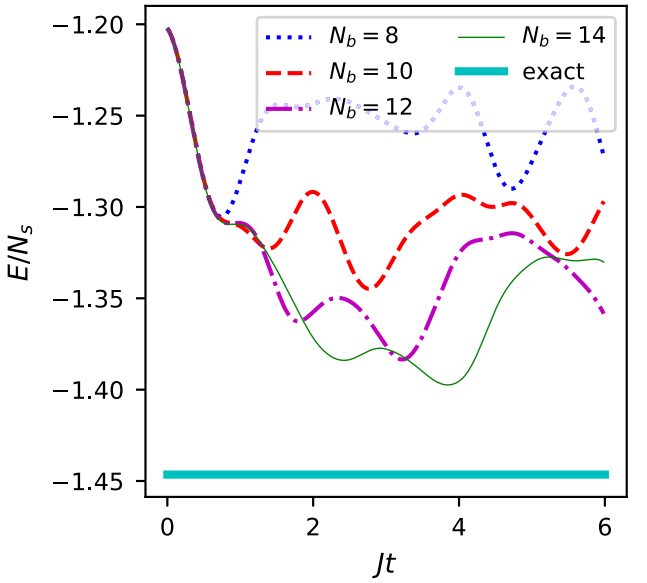

FIG. 3. Energy per site of the state using projective cooling as a function of time in the ordered phase; $J = 1.4$, $n_s = 6$.

III. RESULTS

It is important to first ensure that the system will approach a stable asymptotic state. This can be done by measuring the overlap of the time evolved and projected state with the actual ground state of the Hamiltonian, as done in [12]; however, on a quantum computer it is not possible to measure this overlap. In keeping with the methods of quantum computing we can expect to see asymptotic behavior by measuring the energy density of the projected state in the compact region R_s. The plateau is defined by taking the minimum observed value of the energy density, and then using the calculated values of the energy density earlier in time up to 0.2% above the minimum value to estimate the uncertainty.

Figure 2 shows a typical result ($J = 0.4$ and $N_s = 5$) for the disordered phase. It is clear that the system approaches an approximate plateau for $N_b = 11$ and 13 and less so for $N_b = 9$ and does not approach a plateau at all for $N_b = 7$. Figure 3 demonstrates the evolution toward an asymptotic state in the ordered phase for $J = 1.4$ and $N_s = 6$. The results of the ordered regime are more noisy because there is "heat," in the form of domain wall excitations, leaking back into R_s [18]. This heat is visible from the significant oscillations in energy density over time. The noticeable and important feature that arises is as N_b increases, the minimum of the energy density approaches the exact value. This is reassuring even if we do not see the same plateau. In Fig. 4 ($J = 2.0$ and $N_s = 4$), we see the plateaus become more noticeable again as N_b increases but they are not as clean as the plateaus in the disordered phase.

In Figs. 2, 3, and 4 the energy density of the asymptotic state, in general, becomes closer to the exact energy density as N_b becomes larger. This is indicative that N_b introduces lattice artifacts to the calculation because it is finite. These artifacts can be mitigated by extrapolating to the limit where the volume of R_b is infinite. In order to do this, the following *Ansatz* was chosen:

$$E(N_b) = Ae^{-BN_b} + E_\infty. \tag{7}$$

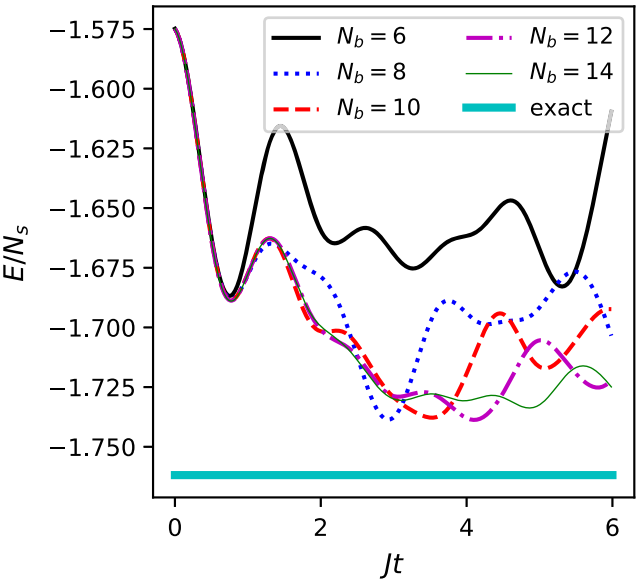

FIG. 4. Energy per site of the state using projective cooling as a function of time in the ordered phase; $J = 2.0$, $n_s = 4$.

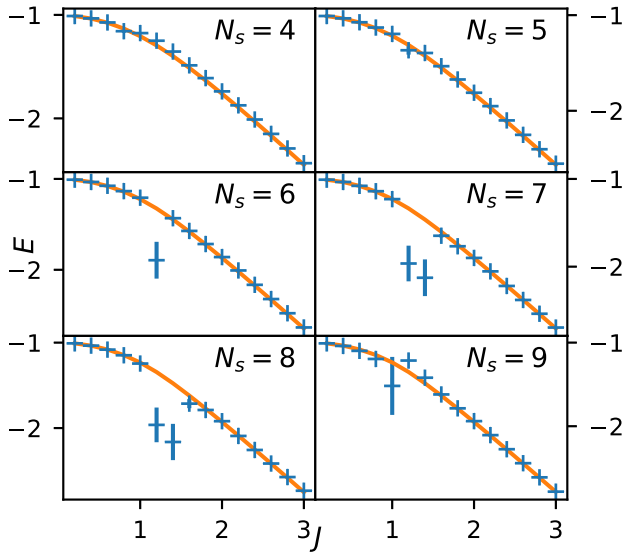

FIG. 5. Energy density using an infinite volume extrapolation as a function of the coupling constant for various compact region sizes. Blue crosses: extrapolated points; orange curve: ground state energy density via exact diagonalization.

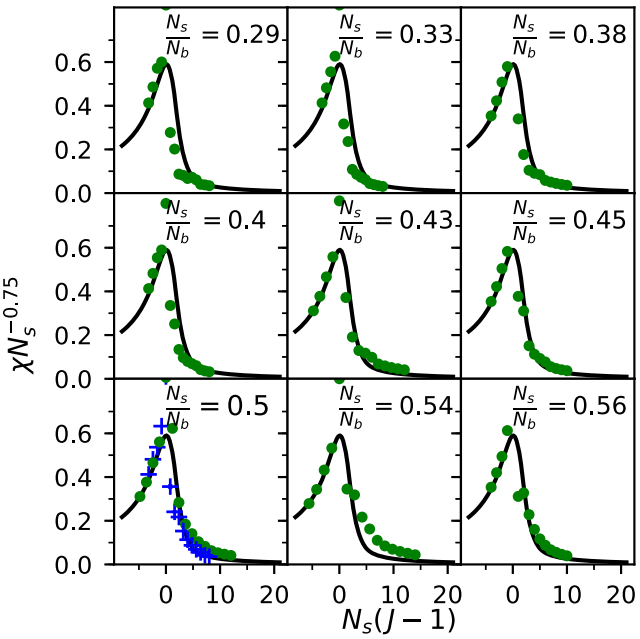

FIG. 6. Rescaled magnetic susceptibility as a function of the rescaled nearest neighbor coupling for various ratios of N_s/N_b. Black curve: interpolation for the exact magnetic susceptibility for 14 sites; green points and blue crosses: calculated susceptibilities using projective cooling.

This *Ansatz* constrains the energy density to always be finite and approach an asymptotic value as $N_b \to \infty$.

The uncertainty in the energy density is calculated by using the data points in the range from the minimal value of the energy density to 2% above the minimal value of the energy density. The result of this algorithm favors simulations that exhibit a plateau verses a local minimum. Figure 5 shows the infinite volume extrapolation. Away from the phase transition ($J = 1$) there is excellent agreement for the energy density in all cases. However for $N_s > 5$, it appears that there is some convergence issues near the phase transition.

A second feature that is indicative that the system is close to the ground state is the finite size scaling relations for the magnetic susceptibility are preserved. The susceptibility is defined as

$$\chi = \frac{1}{N_s}\begin{cases} \sum_{i,j=1}^{N_s}\langle\hat{\sigma}_i^x\hat{\sigma}_j^x\rangle - \langle\hat{\sigma}_i^x\rangle\langle\hat{\sigma}_j^x\rangle & J < h_T \\ \sum_{i,j=1}^{N_s}\langle\hat{\sigma}_i^z\hat{\sigma}_j^z\rangle - \langle\hat{\sigma}_i^z\rangle\langle\hat{\sigma}_j^z\rangle & J \geq h_T \end{cases}, \quad (8)$$

where the different formulas correspond to the different bases that are worked in. The susceptibilities are calculated over the same region that the energy densities are. The data collapse is demonstrated in Fig. 6 where different ratios of N_s/N_b are plotted to demonstrate possible thermal effects. For ratios of $N_s/N_b > 5/9$ nonlinear effects begin to take over and cause the finite size scaling to break down and are not shown.

IV. CONCLUSIONS

This work demonstrates that projective cooling can effectively and accurately prepare the ground state for a relatively simple field theory with a nontrivial ground state. The projective cooling algorithm constructs the ground state in the disordered phase of the transverse Ising model more accurately than in the ordered phase. The discrepancies in the ordered phase are likely a result of thermal effects, indicated by the noticeable discrepancies of the magnetic susceptibility in the ordered phase.

The work done here can be extended to extracting bound states energies for attractive interacting problems such as an Ising-like model with both $\hat{\sigma}^z\hat{\sigma}^z$ and $\hat{\sigma}^x\hat{\sigma}^x$ interactions with only a few changes to the choice of initial state. Other possible extensions could be the Schwinger or O(N) models. In addition, optimizing this algorithm for quantum computation is a challenge that must be addressed as the readout errors and machine noise outside of the R_s can have a drastic effect on the interpreted states and the costs of postselection using the projection operator.

ACKNOWLEDGMENTS

This work was supported in part by the U.S. Department of Energy (DOE) under Award No. DE-SC0019139. I thank Yannick Meurice, Wayne Polyzou, Dean Lee, and Henry Lamm for fruitful conversations.

[1] S. P. Jordan, K. S. M. Lee, and J. Preskill, arXiv:1404.7115.
[2] S. P. Jordan, K. S. M. Lee, and J. Preskill, Quantum Inf. Comput. **14**, 1014 (2011).
[3] E. Farhi, J. Goldstone, S. Gutmann, and M. Sipser, arXiv:quant-ph/0001106.
[4] E. F. Dumitrescu, A. J. McCaskey, G. Hagen, G. R. Jansen, T. D. Morris, T. Papenbrock, R. C. Pooser, D. J. Dean, and P. Lougovski, Phys. Rev. Lett. **120**, 210501 (2018).
[5] A. Peruzzo, J. McClean, P. Shadbolt, M.-H. Yung, X.-Q. Zhou, P. J. Love, A. Aspuru-Guzik, and J. L. O'Brien, Nat. Commun. **5**, 4213 (2014).
[6] A. Roggero, A. C. Y. Li, J. Carlson, R. Gupta, and G. N. Perdue, arXiv:1911.06368.
[7] A. Y. Kitaev, arXiv:quant-ph/9511026.
[8] D. S. Abrams and S. Lloyd, Phys. Rev. Lett. **79**, 2586 (1997).
[9] I. Arad and Z. Landau, SIAM J. Comput. **39**, 3089 (2010).
[10] S. Harmalkar, H. Lamm, and S. Lawrence, arXiv:2001.11490.
[11] H. Lamm and S. Lawrence, Phys. Rev. Lett. **121**, 170501 (2018).
[12] D. Lee, J. Bonitati, G. Given, C. Hicks, N. Li, B.-N. Lu, A. Rai, A. Sarkar, and J. Watkins, arXiv:1910.07708.
[13] J. B. Kogut, Rev. Mod. Phys. **55**, 775 (1983).
[14] J. B. Kogut, Rev. Mod. Phys. **51**, 659 (1979).
[15] J. Zhang, Y. Meurice, and S. W. Tsai, Phys. Rev. A **101**, 033608 (2020).
[16] Y. Meurice, J. Phys. A **40**, R39 (2007).
[17] Using Eq. (3) in ordered regime was found to be worse than using Eq. (4) because domain wall excitations would be stuck in R_s when the system was prepared in the σ^x basis or excitations would bounce back too quickly into R_s for a plataeu to be observed when the system was prepared in the basis of σ^z because N_b was too small.
[18] Attempting to use an eigenstate in the σ^x basis and use (3) for the ordered phase as the disordered phase yielded worse results.